Mechanism for the riddling transition in coupled chaotic systems

Sang-Yoon Kim* and Woochang Lim
Department of Physics, Kangwon National University, Chunchon, Kangwon-Do 200-701, Korea
(Received 4 October 2000; published 25 January 2001)

We investigate the loss of chaos synchronization in coupled chaotic systems without symmetry from the point of view of bifurcations of unstable periodic orbits embedded in the synchronous chaotic attractor (SCA). A mechanism for direct transition to global riddling through a transcritical contact bifurcation between a periodic saddle embedded in the SCA and a repeller on the boundary of its basin of attraction is thus found. Note that this bifurcation mechanism is different from that in coupled chaotic systems with symmetry. After such a riddling transition, the basin becomes globally riddled with a dense set of repelling tongues leading to divergent orbits. This riddled basin is also characterized by divergence and uncertainty exponents, and thus typical power-law scaling is found.

DOI: 10.1103/PhysRevE.63.026217 PACS number(s): 05.45.Xt

I. INTRODUCTION

Recently, the phenomenon of synchronization in coupled chaotic systems has become a field of intensive study. For this case of chaos synchronization, a synchronous chaotic motion of the coupled system occurs on an invariant subspace of the total phase space [1–3]. This chaotic synchronization has a variety of applications, particularly in connection with secure communication [4].

A fundamental and important problem in this field concerns stability of chaos synchronization with respect to a perturbation transverse to the invariant subspace [5]. If its transverse Lyapunov exponent is negative, the synchronous chaotic state on the invariant subspace becomes an attractor in the whole phase space. The loss of transverse stability of such a synchronous chaotic attractor (SCA) is intimately associated with transverse bifurcations of periodic saddles embedded in the SCA [6–8]. When all periodic saddles are transversely stable, the SCA is asymptotically (or strongly) stable (i.e., Lyapunov stable and attracting in the usual topological sense). As the coupling parameter passes through a threshold value, a riddling bifurcation, in which the first periodic saddle embedded in the SCA loses its transverse stability, occurs, and then the SCA becomes weakly stable (i.e., Lyapunov unstable) in the Milnor sense [9]. After the riddling bifurcation, an infinite number of locally repelling ''tongues'' emanate from the transversely unstable repeller and its preimages. Hence, trajectories starting from these tongues will be repelled from the invariant subspace.

However, the fate of the locally repelled trajectories depends on the existence of an absorbing area, controlling the global dynamics, inside the basin of attraction [8,10]. In the case of a supercritical riddling bifurcation, such an absorbing area, acting as a bounded trapping vessel, exists, and hence the locally repelled trajectories exhibit transient intermittent bursting from the invariant subspace [11]. For this case, the basin is said to be locally riddled. However, when the riddling bifurcation is subcritical, there is no absorbing area, and hence the locally repelled trajectories will go to another attractor (or infinity). Thus the basin becomes globally riddled with a dense set of repelling tongues, belonging to the basin of another attractor (or infinity) [12]. With further variation of the coupling parameter, eventually the weakly stable SCA (with locally or globally riddled basin) loses its transverse stability through a blowout bifurcation [13] where the transverse Lyapunov exponent becomes positive, and then it transforms to a chaotic saddle.

In this paper, we investigate the mechanism for the loss of transverse stability of the SCA in terms of unstable periodic orbits embedded in the SCA in a unidirectionally coupled system without symmetry, consisting of one-dimensional (1D) maps. In Sec. II, it is found that a direct transition to global riddling takes place via a transcritical contact bifurcation between a periodic saddle (with one attracting direction and the other repelling direction) embedded in the SCA and a repeller (with two repelling directions) on the basin boundary. Note that this bifurcation mechanism is different from that in coupled chaotic systems with symmetry, where the basin becomes globally riddled through a subcritical pitchfork [6] or period-doubling bifurcation [8]. After the riddling transition, the basin becomes globally riddled with a dense set of tongues leading to divergent trajectories. This riddled basin is a fat fractal with a positive measure [14]. In Sec. III, the measure of the basin riddling and the fine scaled riddling of the fat fractal are also characterized by divergence and uncertainty exponents [15], respectively, and thus typical power-law scaling is found. Finally, a summary is given in Sec. IV.

II. DIRECT TRANSITION TO GLOBAL RIDDLING

In this section, we investigate the loss of transverse stability of the SCA from the point of view of bifurcations of unstable periodic orbits embedded in the SCA, and thus find a mechanism for a direct transition to global riddling through a transcritical contact bifurcation between a periodic saddle embedded in the SCA and a repeller on its basin boundary.

Let us consider the unidirectionally coupled system T without symmetry, consisting of two identical 1D maps,

*Electronic address: sykim@cc.kangwon.ac.kr

$$T:\begin{cases} x_{t+1}=1-ax_t^2, \\ y_{t+1}=1-ay_t^2+c(x_t^2-y_t^2), \end{cases} \tag{1}$$

where x_t and y_t are state variables of the first and second 1D maps at a discrete time t, a is the control parameter of the uncoupled 1D map, and c is a coupling parameter. Note that the unidirectionally coupled map T has an invariant synchronization line $y=x$, although it has no symmetry. This is in contrast to the previously studied case with symmetry [6–8]. Furthermore, this coupled map T is noninvertible, because its Jacobian determinant $\det(DT)$ (DT is the Jacobian matrix of T) becomes zero along the critical curves $L_0=\{(x,y) \in R^2: x=0 \text{ or } y=0\}$. The critical curves of rank k, L_k ($k=1,2,\ldots$), are then given by the images of rank k of L_0 [i.e., $L_k=T^k(L_0)$]. Segments of these critical curves can be used to define a bounded trapping region in the phase plane, called an absorbing area $\mathcal{A}$, with the properties that (i) trajectories that enter $\mathcal{A}$ cannot leave it again, and (ii) there exists a neighborhood $U \supset \mathcal{A}$, whose points enter $\mathcal{A}$ in a finite number of iterations [16]. Furthermore, boundaries of an absorbing area can also be obtained by the union of segments of critical curves and portions of unstable manifolds of unstable periodic orbits. For this case, $\mathcal{A}$ is called a mixed absorbing area.

With increase in the control parameter a, the coupled map T exhibits an infinite sequence of period-doubling bifurcations of synchronous attractors with period 2^n ($n=0,1,2,\ldots$), ending at the accumulation point a_∞ ($=1.401\,155\ldots$), in some region of c. When crossing a critical line in the a-c plane, a transition from periodic to chaotic synchronization occurs. Figure 1 shows the stability diagram for the SCA on the main diagonal ($y=x$), which appears when crossing the critical line, denoted by a heavy solid horizontal line joining two points $c=0$ and $c=-2a_\infty$ on the $a=a_\infty$ line. With further increase of a from a_∞, a sequence of band-merging bifurcations of the SCA take place. For $a=a_n$, the 2^{n+1} bands of the SCA merge into 2^n bands; $a=a_0$ ($=1.543\,689\ldots$), $a=a_1$ ($=1.430\,357\ldots$), and $a=a_2$ ($=1.407\,405\ldots$) lines are shown in the figure. The set of a values yielding synchronous chaotic attractors in the range $(a_\infty,2]$ forms a fat fractal with a positive measure, riddled with a dense set of windows of synchronous periodic attractors [14].

For chaotic values of a, the SCA is at least weakly stable inside the region bounded by solid circles in Fig. 1, because its transverse Lyapunov exponent

$$\sigma_\perp=\lim_{N\to\infty}\frac{1}{N}\sum_{t=1}^{N}\ln\left|\left(1+\frac{c}{a}\right)(-2ax_t)\right| \tag{2}$$

is negative. In periodic windows of a, the solid circles go to the outside (e.g., see the region of the period-3 window near $a\simeq 1.75$). We note that the SCA becomes asymptotically (or strongly) stable in the hatched region with vertical lines, because there all periodic saddles embedded in the SCA are transversely stable. However, when crossing a boundary of the hatched region, this strongly stable SCA becomes weakly stable through a riddling bifurcation, in which the first periodic saddle loses its transverse stability. The solid and dashed boundary lines denote the transverse period-doubling and transcritical bifurcations, which occur when the transverse Floquet (stability) multiplier of the first periodic saddle with period q ($q=1,2,\ldots$),

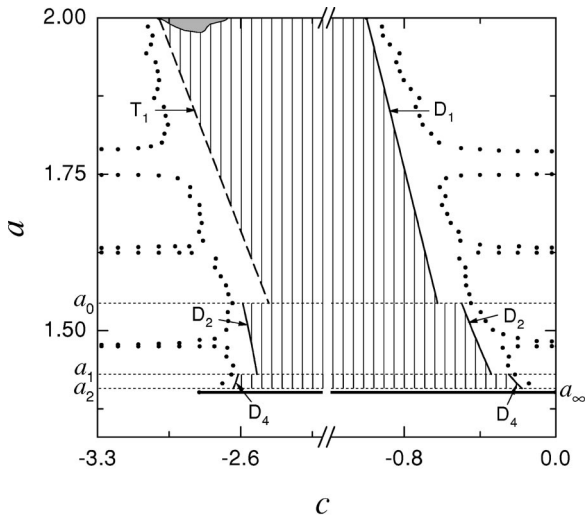

FIG. 1. Stability diagram for the SCA on the diagonal $y=x$ in the a-c plane. The SCA appears when crossing the critical line, denoted by a heavy solid horizontal line on the $a=a_\infty$ ($=1.401\,155\ldots$) line. As a is increased from a_∞, a sequence of band-merging bifurcations occur; some of the band-merging points are a_0 ($=1.543\,689\ldots$), a_1 ($=1.430\,357\ldots$), and a_2 ($=1.407\,405\ldots$). The solid circles denote the points where the transverse Lyapunov exponents of the SCA become zero. T_q and D_q are the riddling bifurcation curves through the transcritical and period-doubling bifurcations of the periodic saddles with period q, respectively. Note that the SCA is strongly stable in the hatched region with vertical lines. In the small gray region near the top of T_1, the basin is also globally riddled due to a boundary crisis between the minimal invariant absorbing of the SCA and its basin boundary. For other details, see the text.

$$\lambda_\perp=\prod_{t=1}^{q}\left(1+\frac{c}{a}\right)(-2ax_t), \tag{3}$$

passes through -1 and $+1$, respectively. These period-doubling and transcritical bifurcation curves of the periodic saddle with period q are also labeled by D_q and T_q, respectively. Some of the riddling bifurcation curves are explicitly shown for $a \geqslant a_2$. For $a \geqslant a_0$, the saddle fixed point with $q=1$, embedded in the SCA with a single band, exhibits a riddling bifurcation. However, as a is decreased from a_0, the SCA becomes a two-band attractor, and then the saddle fixed point lies outside the SCA. Thus, in the range of $a_0 > a \geqslant a_1$, riddling bifurcations occur when the periodic saddle with $q=2$ becomes transversely unstable. In such a way, with further decrease of a, periodic saddles with higher q exhibit riddling bifurcations.

From now on, we discuss the effect of such riddling bifurcations on the SCA. We first note that all but one riddling bifurcation (T_1) are supercritical period-doubling bifurcations (D_q). As shown in coupled chaotic systems with sym-

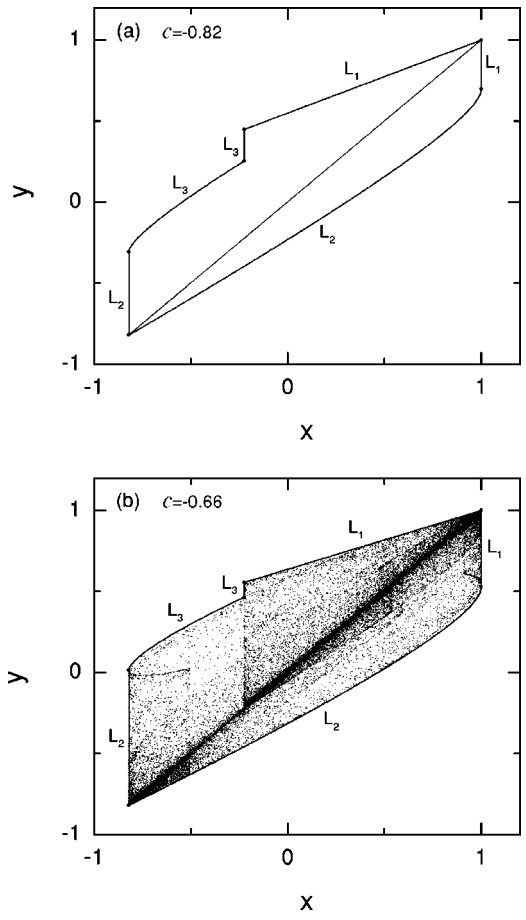

FIG. 2. Global effects of the supercritical riddling and blowout bifurcations for $a=1.82$. (a) After the supercritical riddling bifurcation, an absorbing area, whose boundary is formed by the segments of the critical curves L_1, L_2, and L_3 surrounds the SCA on the diagonal $y=x$ for $c=-0.82$. (b) After the supercritical blowout bifurcation, an asynchronous chaotic attractor, bounded to the absorbing area, exhibits intermittent bursting for $c=-0.66$.

metry [7,8,10], absorbing areas surround the SCA on the diagonal $y=x$ after such supercritical riddling bifurcations. Consequently, the SCA becomes a weakly stable attractor with a locally riddled basin. As an example consider the case of $a=1.82$. A riddling bifurcation occurs when crossing the curve D_1 at $c=c_{r,1}$ $(=-0.850\,625\ldots)$. For this case, the saddle fixed point embedded in the SCA loses its transverse stability through a supercritical period-doubling bifurcation. After that, the SCA is surrounded by an absorbing area, acting as a bounded trapping vessel, as shown in Fig. 2(a) for $c=-0.82$. Hence the locally repelled trajectories exhibit transient intermittent bursting from the synchronization line $y=x$, i.e., the basin becomes only locally riddled. As c is further increased, periodic saddles embedded in the SCA become transversely unstable through successive transverse bifurcations. Eventually, the weakly stable SCA becomes transversely unstable when its transverse Lyapunov exponent becomes positive for $c=c_{b,1}$ $(\simeq -0.677)$, and then it transforms to a chaotic saddle. Since an absorbing area exists, this blowout bifurcation becomes supercritical. Hence, an asynchronous chaotic attractor, bounded to the absorbing area, is developed gradually from the synchronization line $y=x$, as shown in Fig. 2(b) for $c=-0.66$. Near the blowout bifurcation point, such an asynchronous chaotic attractor exhibits a typical intermittent bursting, called the on-off intermittency [17], i.e., the long period of nearly synchronous state (off state) is occasionally interrupted by short-time bursts (on state). As is well known, the average bursting amplitude $\overline{d}$ from the synchronization line is found to increase linearly from zero with respect to Δc $(=c-c_{b,1})$, i.e., $\overline{d}\sim\Delta c$.

However, when crossing the curve T_1, the basin becomes globally riddled with a dense set of tongues, leading to divergent trajectories, through a transcritical contact bifurcation between the saddle fixed point embedded in the SCA and the repeller at the basin boundary. Note that this bifurcation mechanism is different from that in coupled chaotic systems with symmetry [6,8]. For several values of a, we have investigated this riddling transition with variation of the coupling parameter c, and found the same bifurcation mechanism. As an example, consider the case of $a=1.82$. Figure 3 shows the change in the structure of the basin with respect to c. For $c=-2.67$, the SCA is strongly stable, because all periodic saddles embedded in the SCA are stable. The basin for this case is denoted by the gray region in Fig. 3(a). The segments of the unstable manifolds (whose directions are denoted by the arrows) of the repeller, denoted by the down-triangle ($\bigtriangledown$), at the cusp of the basin boundary connect to segments of the critical curves L_1 and L_2 (the dots indicate where these segments connect), and hence define a mixed absorbing area, surrounding the SCA, in which the saddle, denoted by the up-triangle ($\bigtriangleup$), is embedded. As c is decreased, the repeller approaches the saddle, and also the absorbing area shrinks, as shown in Fig. 3(b) for $c=-2.72$. Eventually, at the riddling bifurcation point $c=c_{r,2}$ $(=-2.789\,372\ldots)$, the repeller and saddle collide, and hence the absorbing area disappears [see Fig. 3(c)]. Since the SCA is touching its basin boundary at the saddle point, such a riddling bifurcation induces a contact bifurcation between the SCA and its basin boundary. Note also that an infinitely narrow ''tongue,'' belonging to the basin of an attractor at infinity, opens at the saddle point, as shown in the inset of Fig. 3(c). In fact, the whole basin becomes globally riddled with a dense set of repelling tongues, emanating from the saddle point and its preimages. When passing the point $c_{r,2}$, the repeller moves down off the basin boundary, and exchanges stability with the saddle [i.e., the repeller (saddle) transforms to a saddle (repeller)]. However, the SCA continues to contact its basin boundary at a new repelling fixed point ($\bigtriangleup$). This is just the transcritical contact bifurcation occurring in asymmetric dynamical systems with invariant subspaces when a Floquet multiplier passes 1 [18].

Near the riddling transition point $c=c_{r,2}$, the repelling tongues are too narrow to be observable. For this case, small changes in the dynamical system, destroying its invariant synchronization line $y=x$, lead to superpersistent chaotic transient behavior [19], as in the case of coupled chaotic systems with symmetry [6]. To show this, we introduce a small parameter mismatch by taking the control parameter b of the second 1D map as $b=a-\epsilon$, where a is the control

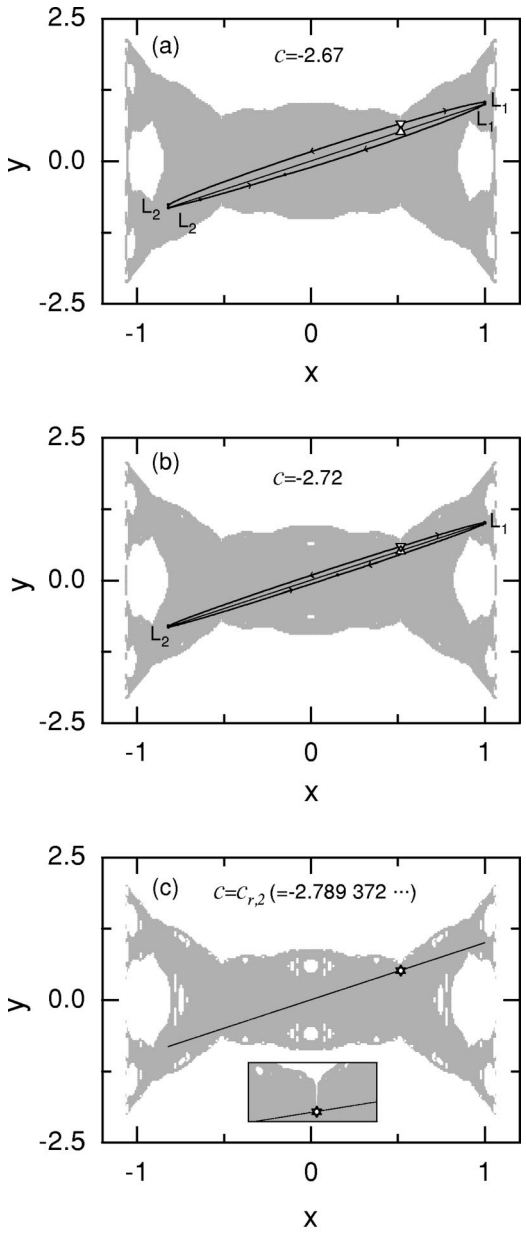

FIG. 3. Change in the structure of the basin (gray region) of the SCA on the diagonal $y=x$ for $a=1.82$. (a) Union of segments of the unstable manifolds of the repeller (∇) at the basin boundary and segments of the critical curves L_1 and L_2 defines a mixed absorbing area of the SCA for $c=-2.67$. (b) As c decreases, the repeller approaches the saddle point ($\triangle$) embedded in the SCA, and hence the absorbing area shrinks, as shown for $c=-2.72$. (c) Through a transcritical contact bifurcation between the repeller (∇) and the saddle point ($\triangle$) for $c=c_{r,2}$, the absorbing area disappears, and then the basin becomes globally riddled with a dense set of tongues, leading to divergent trajectories. For other details, see the text.

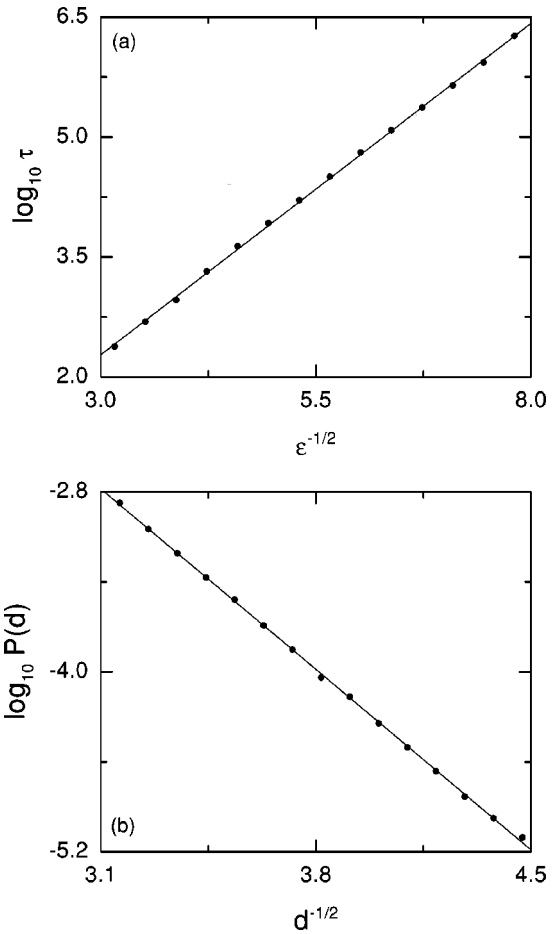

FIG. 4. (a) Plot of $\log_{10}\tau$ (τ is the average lifetime of a chaotic transient) versus $\epsilon^{-1/2}$ (ϵ is the mismatch parameter) for $a=1.82$ and $c=-2.8$. (b) Plot of $\log_{10}P(d)$ [$P(d)$ is the divergence probability] versus $d^{-1/2}$ (d is the distance from the diagonal $y=x$) for $a=1.82$ and $c=-2.8$.

parameter of the first 1D map and ϵ is a small invariance-breaking parameter. When $\epsilon>0$, $y=x$ is no longer an invariant line, and the SCA on the diagonal $y=x$ converts to an extremely long chaotic transient, eventually attracted to infinity. For $c=-2.8$, we decrease ϵ from 0.1 and compute the average transient time. For each value of ϵ, we choose 1000 initial points at random with uniform probability in the range of $x\in(1-a,1)$ on the diagonal $y=x$. A trajectory may be regarded as having escaped once the magnitude of its y value becomes larger than 10, because an orbit point with $|y|>10$ lies sufficiently outside the basin of the SCA. It is thus found that the average lifetime τ of the chaotic transient scales with ϵ as

$$\tau\sim e^{\mu\epsilon^{-\gamma}}, \tag{4}$$

where μ is a positive constant to be fitted, and the exponent γ is 1/2 in contrast to the symmetric-coupling case with $\gamma=2/3$ [6]. Figure 4(a) shows the plot of $\log_{10}\tau$ versus $\epsilon^{-1/2}$ for $0.1\geqslant\epsilon\geqslant0.015$. Note that this plot is well fitted with a straight line, which implies that Eq. (4) is well obeyed. As ϵ decreases toward zero, the average transient time increases faster than any power of ϵ^{-1}. Hence the chaotic transient near $c=c_{r,2}$ is very long lived.

Alternatively, instead of computing the average lifetime of the chaotic transient, we also estimate the variation of the ''divergence'' probability $P(d)$ of being attracted to infinity with the distance d from the synchronization line $y=x$ for

$\epsilon=0$. When $c=-2.8$, decreasing d from 0.1 to 0.05, we compute the divergence probability $P(d)$. For each value of d, we choose an initial condition at random with uniform probability in the range of $x\in(1-a,1)$ on the line $y=x+d$, and determine whether it is attracted to the SCA at $y=x$ or to infinity. We repeat this process until 3000 divergent initial conditions are obtained, and thus estimate $P(d)$. Figure 4(b) shows the plot of $\log_{10}P(d)$ versus $d^{-1/2}$. It is thus found that the divergence probability $P(d)$ scales with d as

$$P(d)\sim e^{-\nu d^{-1/2}}, \tag{5}$$

where ν is a positive constant to be fitted. Note that as d decreases toward zero $P(d)$ decreases more rapidly than any power of d. Hence the measure of the set of repelling tongues is extremely small near the riddling bifurcation point $c=c_{r,2}$.

III. CHARACTERIZATION OF THE RIDDLED BASIN

In the parameter region away from the riddling transition point $c_{r,2}$ for $a=1.82$, we characterize the measure of the basin riddling and the arbitrarily fine scaled riddling of the basin of the SCA by divergence and uncertainty exponents, respectively. As c decreases toward the blowout bifurcation point $c_{b,2}$ ($\simeq-2.963$), the repelling tongues, leading to divergent trajectories, continuously expand, as shown in Figs. 5(a), 5(b), and 5(c), and hence the measure of the riddled basin of the SCA decreases to zero. Finally, on passing the blowout bifurcation point $c_{b,2}$, a subcritical blowout bifurcation, leading to the abrupt collapse of the synchronized state, occurs. For this subcritical case, there is no absorbing area, and hence typical trajectories starting near the synchronization line $y=x$ diverge to infinity, in contrast to the supercritical case where an asynchronous chaotic attractor is gradually developed from the synchronization line.

We first characterize the measure of the basin riddling (i.e., the measure of the set of repelling tongues, leading to divergent trajectories) by the variation of the divergence probability $P(d)$ of being attracted to the infinity [15] with the distance d from the synchronization line $y=x$. Near the riddling bifurcation point ($c\simeq c_{r,2}$), $P(d)$ exhibits the exponential scaling of Eq. (5), because the measure of the set of repelling tongues is extremely small. However, a transition from exponential to algebraic scaling occurs when passing a crossover region ($-2.84\lesssim c\lesssim-2.81$). Thus, for $c\lesssim-2.84$, the divergence probability $P(d)$ scales with d as

$$P(d)\sim d^{\eta}, \tag{6}$$

where η is referred to as the divergence exponent. As the value of η becomes smaller, it becomes easier for trajectories starting near the synchronization line to go to infinity. For a given value of c, we take many randomly chosen initial conditions on the line $y=x+d$ and determine which basin they lie in. Then, $P(d)$ is estimated as the fraction of the points that are attracted to infinity. When plotting $\log_{10}P(d)$ versus $\log_{10}d$, the slope of the fitted straight line gives the value of the divergence exponent η. Figure 6(a) shows the plot of η versus c for $-2.96\leqslant c\leqslant-2.85$. With decrease in c toward the blowout bifurcation point $c_{b,2}$, the value of η becomes smaller, and hence the measure of the basin riddling increases.

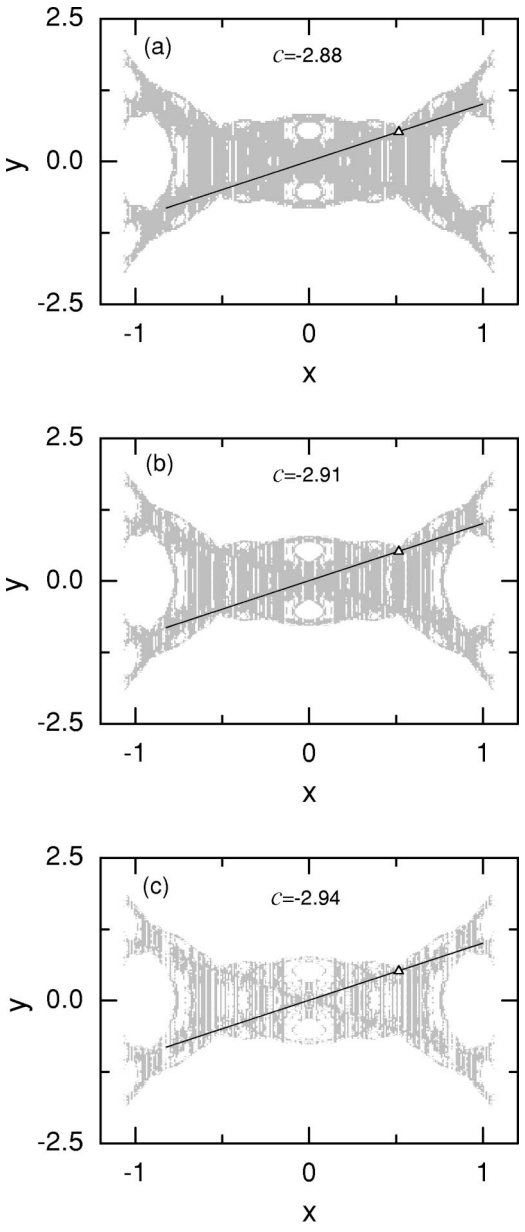

FIG. 5. Globally-riddled basins (gray region) of the SCA on the diagonal $y=x$ for (a) $c=-2.88$, (b) $c=-2.91$, and (c) $c=-2.94$. As c decreases toward the blowout bifurcation point $c_{b,2}$ ($\simeq-2.963$), the measure of the set of repelling tongues (shown white) increases, and hence the measure of the riddled basin decreases to zero.

The results of Eq. (6) give just the measure of the basin riddling, but the equation says nothing about the arbitrarily fine scaled riddling of the basin of the SCA. The riddled basin of the SCA is a fat fractal. The fine scaled riddling of the fat fractal is also characterized by an uncertainty exponent α [15] on decreasing c from -2.85 to -2.96. For a given c, consider a square with sides of length 0.3, centered

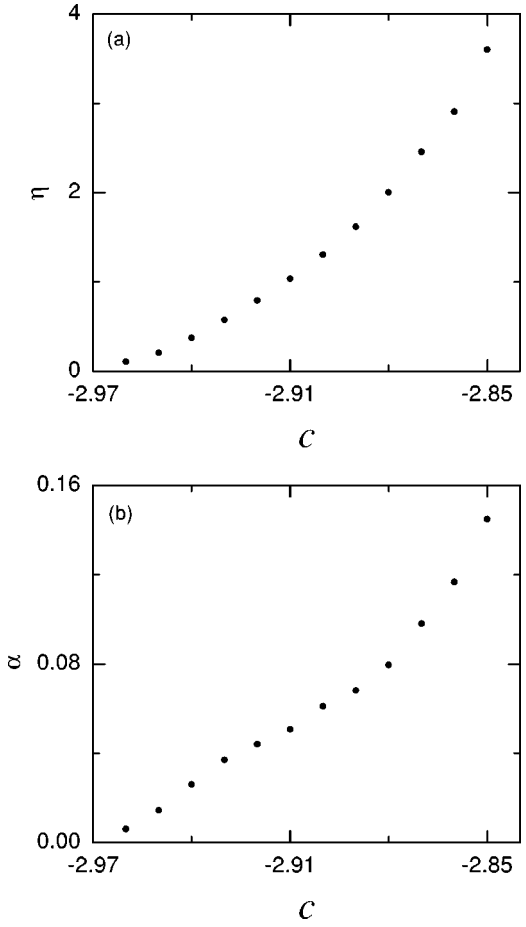

FIG. 6. (a) Plot of the divergence exponent η versus c for $a=1.82$. (b) Plot of the uncertainty exponent α versus c for $a=1.82$.

at a point $(0.35,0.35)$. We first choose a point z at random with uniform probability inside the square. We also choose a second point z' at random within a small square with sides of length 2ϵ, centered at the first point z. Then we determine the final states of the trajectories starting with the two initial conditions z and z'. If the final states are different, the initial point z is said to be uncertain. We repeat this process for a large number of randomly chosen initial conditions until 4000 uncertain initial conditions are obtained, and estimate the probability $P(\epsilon)$ that the two initial conditions z and z' yield different final states. With decreasing ϵ, $P(\epsilon)$ exhibits a power-law scaling,

$$P(\epsilon)\sim\epsilon^{\alpha}, \tag{7}$$

where α is referred to as the uncertainty exponent. Note that, if $\alpha<1$, then a substantial improvement in the accuracy of the initial conditions yields only a small decrease in the uncertainty of the final state. Figure 6(b) shows the plot of α versus c for $-2.96\leqslant c\leqslant -2.85$. As c decreases toward the blowout bifurcation point $c_{b,2}$, the value of α becomes smaller, and hence the uncertainty in determining the final state increases.

IV. SUMMARY

We have investigated the loss of chaos synchronization in terms of unstable periodic orbits embedded in the SCA in unidirectionally and nonlinearly coupled 1D maps, and found a mechanism for the transition to global riddling through a transcritical contact bifurcation between a periodic saddle embedded in the SCA and a repeller on its basin boundary. This bifurcation mechanism was also confirmed in the linearly coupled case [20]. We thus believe that it is a generic bifurcation mechanism leading to a direct transition to global riddling in unidirectionally coupled systems without symmetry. Note that this bifurcation mechanism is different from that in coupled chaotic systems with symmetry [6,8]. As a result of the riddling transition, the basin becomes globally riddled with a dense set of tongues, leading to divergent trajectories. This riddled basin has also been characterized by divergence and uncertainty exponents, and thus typical power-law scaling has been found.

ACKNOWLEDGMENT

This work was supported by the Korean Research Foundation under Grant No. 2000-041-D00067.

[1] H. Fujisaka and T. Yamada, Prog. Theor. Phys. **69**, 32 (1983).
[2] A.S. Pikovsky, Z. Phys. B: Condens. Matter **50**, 149 (1984).
[3] L.M. Pecora and T.L. Carroll, Phys. Rev. Lett. **64**, 821 (1990).
[4] K.M. Cuomo and A.V. Oppenheim, Phys. Rev. Lett. **71**, 65 (1993); L. Cocarev, K.S. Halle, K. Eckert, L.O. Chua, and U. Parlitz, Int. J. Bifurcation Chaos Appl. Sci. Eng. **2**, 973 (1992); L. Kocarev and U. Parlitz, Phys. Rev. Lett. **74**, 5028 (1995); N.F. Rulkov, Chaos **6**, 262 (1996).
[5] P. Ashwin, J. Buescu, and I. Stewart, Nonlinearity **9**, 703 (1996).
[6] Y.-C. Lai, C. Grebogi, J.A. Yorke, and S.C. Venkataramani, Phys. Rev. Lett. **77**, 55 (1996).
[7] V. Astakhov, A. Shabunin, T. Kapitaniak, and V. Anishchenko, Phys. Rev. Lett. **79**, 1014 (1997).
[8] Yu.L. Maistrenko, V.L. Maistrenko, A. Popovich, and E. Mosekilde, Phys. Rev. E **57**, 2713 (1998); **60**, 2817 (1999).
[9] J. Milnor, Commun. Math. Phys. **99**, 177 (1985).
[10] Yu.L. Maistrenko, V.L. Maistrenko, A. Popovich, and E. Mosekilde, Phys. Rev. Lett. **80**, 1638 (1998); G.-I. Bischi and L. Gardini, Phys. Rev. E **58**, 5710 (1998).
[11] P. Ashwin, J. Buescu, and I. Stewart, Phys. Lett. A **193**, 126 (1994); J.F. Heagy, T.L. Carroll, and L.M. Pecora, Phys. Rev. E **52**, 1253 (1995); S.C. Venkataramani, B.R. Hunt, E. Ott, D.J. Gauthier, and J. C. Bienfang, Phys. Rev. Lett. **77**, 5361 (1996); S.C. Venkataramani, B.R. Hunt, and E. Ott, Phys. Rev. E **54**, 1346 (1996).
[12] J.C. Alexander, J.A. Yorke, Z. You, and I. Kan, Int. J. Bifurcation Chaos Appl. Sci. Eng. **2**, 795 (1992); E. Ott, J.C. Sommerer, J.C. Alexander, I. Kan, and J.A. Yorke, Phys. Rev. Lett.

71, 4134 (1993); J.C. Sommerer and E. Ott, Nature (London) **365**, 136 (1993); E. Ott, J.C. Alexander, I. Kan, J.C. Sommerer, and J.A. Yorke, Physica D **76**, 384 (1994).

[13] E. Ott and J.C. Sommerer, Phys. Lett. A **188**, 39 (1994).

[14] J.D. Farmer, Phys. Rev. Lett. **55**, 351 (1985).

[15] E. Ott, J.C. Sommerer, J.C. Alexander, I. Kan, and J.A. Yorke, Phys. Rev. Lett. **71**, 4134 (1993); E. Ott, J.C. Alexander, I. Kan, J.C. Sommerer, and J.A. Yorke, Physica D **76**, 384 (1994); J.F. Heagy, T.L. Caroll, and L.M. Pecora, Phys. Rev. Lett. **73**, 3528 (1994).

[16] C. Mira, L. Gardini, A. Barugola, and J.-C. Cathala, *Chaotic Dynamics in Two-Dimensional Noninvertible Maps* (World Scientific, Singapore, 1996); R.H. Abraham, L. Gardini, and C. Mira, *Chaos in Discrete Dynamical systems* (Springer, New York, 1997).

[17] H. Fujisaka and T. Yamada, Prog. Theor. Phys. **74**, 918 (1985); N. Platt, E.A. Spiegel, and C. Tresser, Phys. Rev. Lett. **70**, 279 (1993); J.F. Heagy, N. Platt, and S.M. Hammel, Phys. Rev. E **49**, 1140 (1994).

[18] J. Guckenheimer and P. Holmes, *Nonlinear Oscillations, Dynamical Systems, and Bifurcations of Vector Fields* (Springer, New York, 1983), p. 149.

[19] C. Grebogi, E. Ott, and J.A. Yorke, Phys. Rev. Lett. **50**, 935 (1983); Ergod. Theory Dyn. Syst. **5**, 341 (1985).

[20] S.-Y. Kim and W. Lim (unpublished).